A General Time-Domain Method for Harmonic Distortion Estimation in CMOS Circuits

Dimitrios Baxevanakis, *Graduate Student Member, IEEE*, and Paul P. Sotiriadis, *Senior Member, IEEE*

***Abstract*—This article presents a general, time-domain harmonic distortion estimation method, applicable to linear CMOS circuits characterized by weakly nonlinear behavior, ranging from amplifiers, and transconductors to filters, with any number of stages. It offers a compact, fast, and systematic way to model circuits as a structure of interconnected G_m-stages, and estimates the harmonic distortion at every circuit node, providing insight into the distortion contribution of every stage. The method uses a more involved model for each G_m-stage that also accounts for the dependence of its output current on cross-products of its input and output voltages, improving significantly the distortion estimation accuracy. The proposed method is easily implemented in MATLAB, and intends to be integrated as a tool in EDA suites to speed-up distortion estimation. A number of examples are presented, illustrating the application of the method and validating its accuracy via comparison with Cadence Spectre simulation.**

***Index Terms*—CMOS, estimation, G_m-stage, linear circuits, total harmonic distortion (THD), weak nonlinearities.**

I. Introduction

HARMONIC distortion is an important aspect in characterizing a circuit's performance. Harmonic distortion and noise determine its dynamic range [1], whereas alongside with intermodulation distortion they dictate the circuit's overall linearity. As such, it is a quantity of major impact and interest in a plethora of applications, like audio and power amplifiers [2], radio-frequency amplifiers [3], low-noise amplifiers, filters, and more.

Supposing that a circuit is being driven by a sinusoidal signal of fundamental frequency ω, the total harmonic distortion (THD) at its output is defined as the ratio of the combined power of all generated harmonics to the power of the fundamental

$$\mathrm{THD} = \sqrt{\frac{\sum_{k=2}^{\infty} V_{h_k}^2}{V_f^2}} \cdot 100\%. \tag{1}$$

V_{h_k} is the (voltage) amplitude of the kth harmonic, at frequency $k\omega$, and V_f is the amplitude of the fundamental tone.

Manuscript received January 22, 2020; revised March 12, 2020; accepted March 25, 2020. Date of publication April 16, 2020; date of current version January 11, 2021. This work was supported in part by Greece and the European Union (European Social Fund–ESF) through the Operational Programme "Human Resources Development, Education and Lifelong Learning" in the context of the Project "Strengthening Human Resources Research Potential via Doctorate Research" under Grant MIS-5000432, implemented by the State Scholarships Foundation (IKY), and in part by the Scholars' Association of the Alexander S. Onassis Public Benefit Foundation, Greece. This article was recommended by Associate Editor N. Wong. *(Corresponding author: Dimitrios Baxevanakis.)*

The authors are with the Department of Electrical and Computer Engineering, National Technical University of Athens, 157 80 Athens, Greece (e-mail: dimbaxev@central.ntua.gr; pps@ieee.org).

Digital Object Identifier 10.1109/TCAD.2020.2988414

Realistically, under weakly nonlinear circuit behavior, the harmonic amplitudes decrease rapidly as their order increases, which in turn significantly decreases the number of harmonics needed to have a good estimation of THD. Depending on the specific circuit topology, the dominant harmonic tones are the second and the third harmonic. This raises interest in determining the HD_2 and HD_3 distortion factors

$$\mathrm{HD}_2 = \left|\frac{V_{h_2}}{V_f}\right|, \quad \mathrm{HD}_3 = \left|\frac{V_{h_3}}{V_f}\right| \tag{2}$$

that are the estimation subjects of this article.

Accurate prediction of distortion is, in general, a complicated task. A possible way of estimating the distortion in a circuit is by simulation. A sinusoidal input results in sinusoidal currents and voltages of the same frequency (assuming no chaotic behavior or subharmonic generation), and so simulation methods like harmonic balance or shooting [4], [5], are most appropriate. Unfortunately, the estimation of distortion by such methods is usually time-consuming and computationally expensive [6], does not provide any insight [7], and does not aid with optimization or parameterization of the design.

Dedicated methods that predict the distortion behavior and are easy to use, while being open to parameterization and provide insight are sought after. A popular approach is by means of the Volterra series [8], where the circuit is decomposed into various order operators, each one characterized by a time- or frequency-domain Volterra kernel. Even though the use of the Volterra series can yield quite accurate results, there are shortcomings; the operators' expression and manipulation becomes cumbersome when the number of circuit elements (and thus, distortion contributions) rises, which is almost always the case for practical circuits.

Recently, a methodology utilizing linear-centric circuit models to account for individual distortion contributions in a circuit was reported [9]. Systematic, time-domain state-space harmonic distortion estimation approaches for weakly nonlinear G_m-C filters of any order [10]–[12], and a distortion contribution analysis that uses the best linear approximation [13] were also proposed; the latter methodology deviates from the classical distortion point of view and adopts a noise-like analysis, being also capable of handling strong nonlinearities.

Several other methods describe the dominant distortion terms in the frequency-domain [14], [15], where many use algebraic manipulation of simplified amplifier models [16]–[24]. The analysis is mainly focused on the most frequently used amplifier topologies, with one, two, or three stages, employing negative feedback and Miller compensation. Even though some share similarities with the Volterra series approach [25], or adopt them [3], [15], they provide a set of equations ready to be used. However, most works are usually tailored for specific topologies, and may require extensive algebraic manipulation to be applied to more general cases.

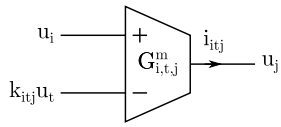

Fig. 1. G_m-stage representation.

Additionally, the models used in many of these approaches could fail to capture faithfully the current-characteristic of a CMOS stage, as will be demonstrated in the sections to follow.

This article extends [26] and proposes a general, time-domain harmonic distortion estimation method for CMOS circuits that exhibit weak nonlinearities. It offers a compact and systematic approach that can be applied to circuit structures ranging from simple transconductors to cascaded amplifiers and filter designs, with any number of stages. It provides a fast and highly accurate estimation of distortion factors HD_2 and HD_3 by manipulating the circuit under consideration as a structure of interconnected G_m-stages. Each G_m-stage is characterized by a more involved model of its current-characteristic, whose parameters are extracted via curve-fitting. The method is easily implemented in numerical computing environments like MATLAB, and intends to serve as an integrated tool in dedicated EDA software (like Cadence Spectre) to speed-up distortion estimation.

The remainder of this article is organized as follows. Section II presents the modeling of CMOS stages, and Section III outlines the derivation of the G_m-stage model coefficients. Section IV introduces the proposed method alongside with examples of its application, while the method's accuracy is validated through simulation results in Section V. Finally, conclusions are drawn in Section VI.

II. Gm-Stage Modeling

A MOS transistor eventually constitutes a voltage-controlled current source. In the same vein, a CMOS gain stage producing an output current in response to an input voltage can be thought of as a G_m-stage, a representation of which is depicted in Fig. 1.

Throughout this article, the following notation is used; $G^m_{i,t,j}$ is the G_m-stage with positive input, u_i, at node i; negative input, $k_{itj}u_t$, from node t, with k_{itj} a real feedback factor[1]; and output current, i_{itj}, at node j. The stage's differential input voltage is then

$$\widetilde{u}_{itj} = u_i - k_{itj}u_t. \tag{3}$$

The itj-triplet[2] is included in all of the characteristics of a G_m-stage. The ac-ground is marked as r (reference potential).

For keeping the expressions and notation as simple as possible, single-ended output G_m-stages were preferred. This, however, does not limit the application of the proposed method, as fully-differential circuits can be easily modeled by single-ended output G_m-stages, as described later in Section II-D2.

A stage's output current is in general a nonlinear function of its input and output voltages

$$i_{itj} = f_{i,t,j}\big(\widetilde{u}_{itj}, u_j\big), \quad f_{i,t,j} : \mathbb{R}^2 \to \mathbb{R}. \tag{4}$$

This nonlinearity is the cause of distortion generation.

[1]This particular notation is adopted to capture a range of popular topologies.

[2]Commas between i, t, and j are omitted in coefficients, voltages, and currents for simplicity.

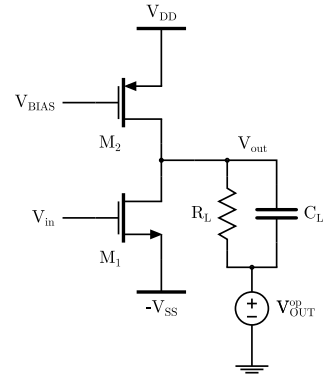

Fig. 2. CS amplifier.

Parasitic capacitors in MOS transistors are reported to do not have significant nonlinearity contribution; they reduce the magnitude of the output impedance at high frequencies [27], [28]. This enables the formation of an equivalent model based only on the dc-characteristics of a CMOS stage. Such a model can be obtained by approximating the stage's output current with a power-series expansion around its dc-operating point.

A. Simple Model

The simplest case results by neglecting the output voltage dependence and modeling the whole stage as a single current source that is governed by power terms of its input voltage

$$i_{itj} = \sum_{k\geq 1} g_{itj,k}\widetilde{u}^k_{itj} \tag{5}$$

where $g_{itj,k}$ is the corresponding coefficient for each power, k, of $\widetilde{u}^k_{itj}$. This approach, however, will result in poor accuracy since it even fails to account for the finite output impedance of the stage. As such, a better approximation has to be made.

B. More Accurate Model

The most frequently adopted approach [17], [18], [20]–[23] is to take into account both the input and output voltages and have a power-series approximation of the form

$$i_{itj} = \sum_{k\geq 1}\Big(g_{itj,k}\widetilde{u}^k_{itj} + \overline{g}_{itj,k}u^k_j\Big). \tag{6}$$

Since HD_2 and HD_3 are the dominant distortion factors, one can restrict $k = 1, 2, 3$ to end up with an easy to manipulate and fairly accurate expression.[3] An additional advantage of this approximation is that the input- and output-related terms are independent of one another; nonetheless, this can lead to significant deviations in the expected behavior of a G_m-stage.

To illustrate such a case, consider the common-source (CS) amplifier of Fig. 2. Its load, $R_L \| C_L$, has a reference voltage of V^{op}_{OUT}, the dc-operating point of the unloaded output.

Should the input and output voltages be independent, the circuit of Fig. 3 must produce the same distortion. The original CS stage is mirrored, isolating the interference between the input and output voltages; V_{in} acts under a fixed V^{op}_{OUT} and produces a current signal, i_{sig}; this signal is in turn injected

[3]Including higher-order terms will account better for distortion expansion and compression at the harmonics of interest; however, since weak nonlinearities are assumed, the error will be negligible.

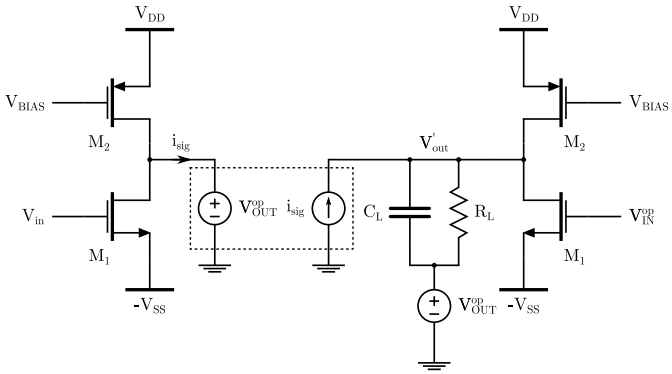

Fig. 3. CS amplifier—independent input and output voltages.

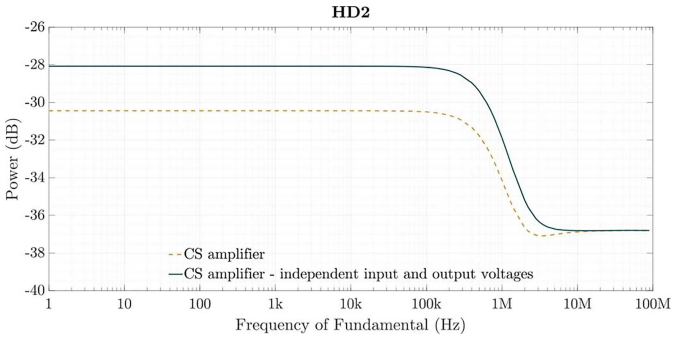

Fig. 4. HD_2 of the two CS amplifier cases.

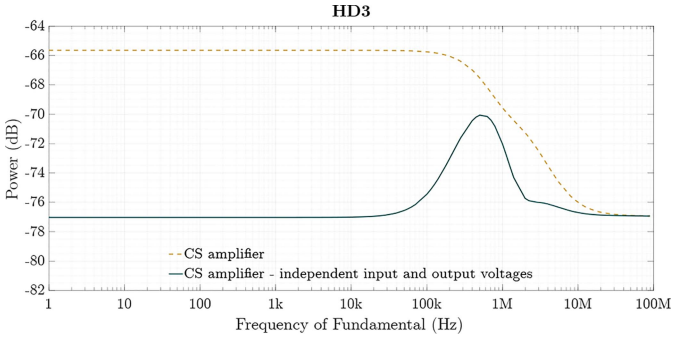

Fig. 5. HD_3 of the two CS amplifier cases.

into the output node of the mirror-stage (operating under V_{IN}^{op}, the input dc-operating point of Fig. 2), creating V'_{out}.

The two cases were simulated by means of Cadence Spectre in TSMC 0.18 μm technology. The amplifier has a dc-gain of 14.7 dB under a load of 10 k$\Omega\|$ 10 pF, and a unity-gain frequency of 9.35 MHz. A parametric (with respect to frequency) periodic steady-state (PSS) harmonic balance analysis is performed, with a sinusoidal input signal of 50 mV peak. The resulting HD_2 and HD_3 are presented in Figs. 4 and 5, respectively. It is evident that the two circuits exhibit different distortion mechanisms, even though they have the same fundamental frequency response. Similar findings on the importance of input-output related terms have been recently reported [15].

C. Proposed Model

Given the drawbacks of the previous approach, it is fair to say that a suitable model should also include cross-products of the input and output voltages. Such approximations have been

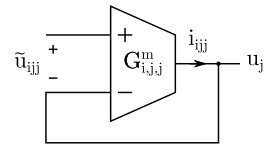

Fig. 6. SF stage as a G_m-stage.

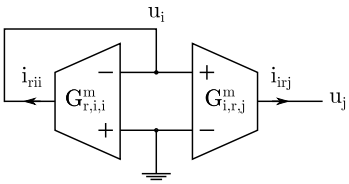

Fig. 7. CG stage as a G_m-stage.

used at transistor-level [3], [27]–[30], where the device acting as amplifier is supposed to admit a 2- or 3-D Taylor series expansion; the corresponding coefficients of the approximation are then calculated by the partial derivatives of the transistor's current relationship. Equivalent approaches have been adopted at stage-level [3], [14], [15], [31]–[33].

In this article, each G_m-stage is considered to have a time-domain [10]–[12], [34] power-series current expression

$$i_{itj} = \sum_{\substack{k,\ell\geq 0\\ k+\ell\geq 1}} g_{itj}^{k\ell}\widetilde{u}_{itj}^{k}u_j^{\ell}. \tag{7}$$

Note that for notation simplicity, the $k\ell$-superscript in the $g_{itj}^{k\ell}$-coefficients indicates the corresponding power of $\widetilde{u}_{itj}^{k}$ and u_j^{ℓ}, and not a power term of the coefficient itself.

It is chosen that $k+\ell = 1, 2, 3$, to capture the dominant contributing terms to the fundamental, second and third harmonic, and (7) reduces to

$$\begin{aligned} i_{itj} = {} & g_{itj}^{10}\widetilde{u}_{itj} + g_{itj}^{20}\widetilde{u}_{itj}^{2} + g_{itj}^{30}\widetilde{u}_{itj}^{3} \\ & + g_{itj}^{01}u_j + g_{itj}^{02}u_j^{2} + g_{itj}^{03}u_j^{3} \\ & + g_{itj}^{11}\widetilde{u}_{itj}u_j + g_{itj}^{21}\widetilde{u}_{itj}^{2}u_j + g_{itj}^{12}\widetilde{u}_{itj}u_j^{2}. \end{aligned} \tag{8}$$

The $g_{itj}^{k\ell}$-coefficients of (8) of each G_m-stage are derived by curve-fitting to capture in detail its amplitude-adjusted nonlinearities. Taylor series expansion at the dc-operating point (used in most of the aforementioned works and employed in various analyses) is accurate only locally for small signal amplitudes [35]. The derivation procedure of the $g_{itj}^{k\ell}$-coefficients is described analytically in Section III.

D. Formulation of Standard CMOS Gain Stages

The formulation of a CMOS gain stage depends on its topology, and thus, whether it is single-ended or fully-differential.

1) Single-Ended Structures: The differential-pair can be modeled directly in the form of Fig. 1. For a CS stage, the negative input should be ac-grounded; a source-follower (SF) stage should be treated as a G_m-stage with 100% negative feedback ($k_{ijj} = 1$), as shown in Fig. 6.

A common-gate (CG) stage is modeled as depicted in Fig. 7, where antiparallel stages $G_{i,r,j}^{m}$ and $G_{r,i,i}^{m}$ have the same $g_{itj}^{k\ell}$-coefficients. This formulation results from the fact that in a CG stage the output current flows toward its input source.

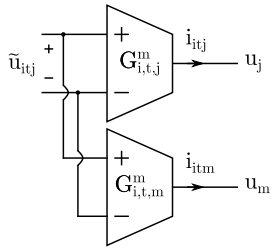

Fig. 8. Fully-differential structure G_m-stage representation.

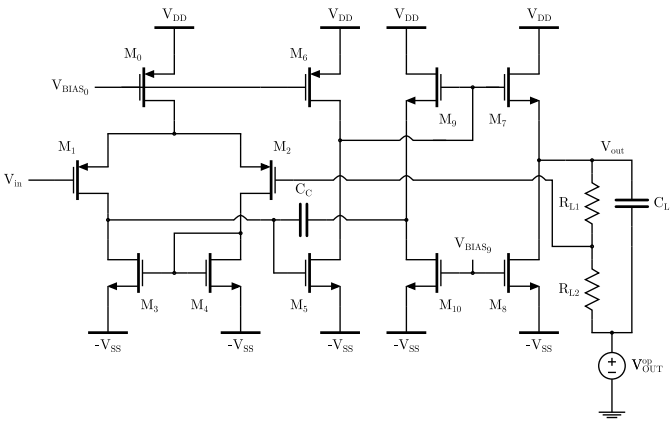

Fig. 9. Three-stage feedback amplifier.

Stages that result from combinations of the aforementioned standard ones can be represented as connections of their G_m-stage equivalents, or even be treated as a single G_m-stage. An example of the latter case is presented in Section IV-E1.

2) Fully-Differential Structures: In the case of a fully-differential stage, an appropriate representation would be that of Fig. 8. The two G_m-stages are connected with their inputs in parallel, and each set of $g^{k\ell}_{itj}$-coefficients results from the common input and the corresponding output. Ideally, $g^{k\ell}_{itm} = -g^{k\ell}_{itj}$, so as to achieve $i_{itm} = -i_{itj}$.

E. Circuit Transformation Into a G_m-Stage Equivalent

The transformation of a circuit into an equivalent representation of G_m-stages relies on identifying the standard CMOS gain stages that it is comprised of, and their interconnections.

As an example, consider the three-stage feedback amplifier of Fig. 9. The amplifier consists of three cascaded stages (differential-pair, CS, SF) and a buffer stage (SF) for Miller compensation.

The equivalent representation of the amplifier is that of Fig. 10. Transistors M_0–M_4 of the differential-pair form the first G_m-stage, $G^m_{0,3,1}$, while the CS stage of M_5–M_6 forms the second stage, $G^m_{1,r,2}$. The SF stage of M_7–M_8 forms $G^m_{2,3,3}$, and the SF stage of M_9–M_{10} forms $G^m_{2,4,4}$. Moreover, it is $k_{233} = k_{244} = 1$, as described in Section II-D1.

The negative input of the differential-pair (and thus, $G^m_{0,3,1}$) is fed with an ac-voltage of

$$\frac{R_{L_2}}{R_{L_1} + R_{L_2}} u_{\text{out}} = k_{031} u_{\text{out}} = k_{031} u_3$$

where $R_{L_1} + R_{L_2} = R_L = R_3$. Finally, $C_L = C_3$ and $C_C = \widetilde{C}_{14}$. The ac-input signal, $u_{in} = u_0$, is realized by the current

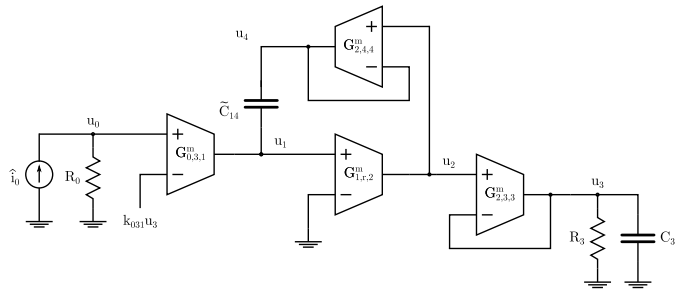

Fig. 10. G_m-stage equivalent representation of the three-stage feedback amplifier.

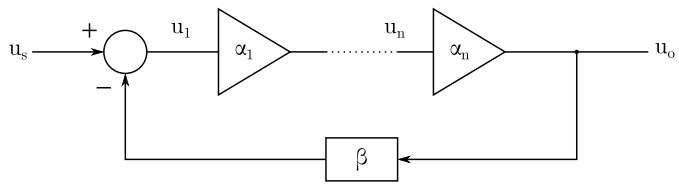

Fig. 11. Closed-loop system configuration.

source $\hat{i}_0 = u_0/R_0$ that acts on the normalized[4] $R_0 = 1\,\Omega$; this transformation results from the method's formulation that is presented in Section IV.

III. Model Coefficients Derivation

The derivation of the $g^{k\ell}_{itj}$-coefficients of each G_m-stage model can be performed by a three-step procedure that involves an ac-analysis performed to the whole circuit structure, 2-D dc-sweeps around the input and output dc-operating points of each stage, and, finally, linear regression for the estimation of the coefficients. The findings of this procedure should confirm weakly nonlinear behavior for all G_m-stages, otherwise the method's accuracy will be degraded.

A. AC-Analysis for Amplitude Levels Estimation

An ac-analysis is initially performed to the complete circuit under consideration, to gain knowledge about the expected signal amplitude at the input and the output of each stage.

The input and output amplitudes of a stage with respect to the circuit's input signal can deviate from an anticipated monotonous drop in open-loop applications as frequency rises. When the circuit is in closed-loop configuration, the maximum value may be achieved at higher frequencies. In the system representation of Fig. 11, the gain from the input signal, u_s, to the input of the first stage, u_1, is

$$\frac{u_1}{u_s} = \frac{1}{1 + \beta\alpha_1 \cdots \alpha_n}. \tag{9}$$

As the gain of each stage falls with frequency, the gain to the input of the first stage rises, and so does its input amplitude. Depending on the gains $\alpha_1, \ldots, \alpha_n$, and whether additional feedback exists, more stages can exhibit similar behavior.

Figs. 12 and 13 depict the gains u_1/u_s, u_2/u_s, and u_3/u_s, for the differential-pair and the CS stage, respectively, of the feedback amplifier of Fig. 9. Let the differential-pair's differential input voltage be denoted by u_1 and its output voltage

[4]If the input signal source drives a CG stage, R_0 must be significantly smaller in value than the input impedance of the stage.

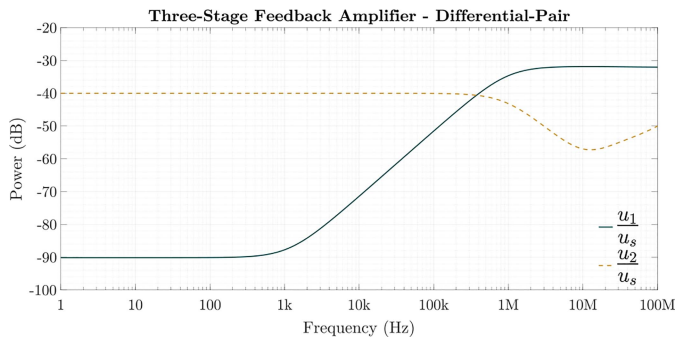

Fig. 12. Gains u_1/u_s and u_2/u_s for the differential-pair.

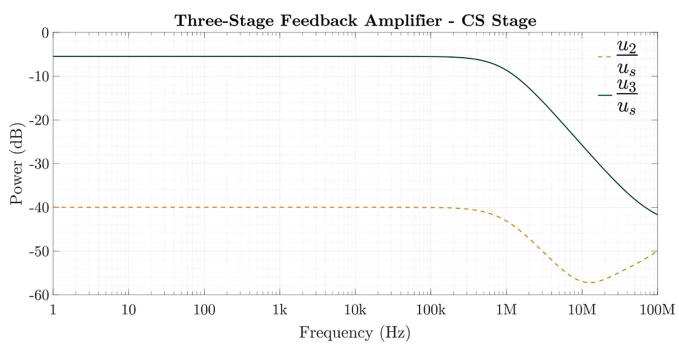

Fig. 13. Gains u_2/u_s and u_3/u_s for the CS stage.

by u_2; accordingly, the CS stage has u_2 as input voltage and u_3 as output voltage. Whereas both gains reach their maximum value at low frequencies in the CS stage, the gain of the input of the differential-pair starts to rise and reaches its peak higher in frequency, but well inside the amplifier's unity-gain bandwidth of 16.80 MHz. The simulations were done again with Cadence Spectre in TSMC 0.18 μm technology.

B. 2-D DC-Sweeps for Current-Characteristics

The derived maximum values (within the bandwidth of interest for the distortion estimation), when referred back to the excitation signal, mark the peak amplitudes that the input and the output of a stage will confront. As such, they are the ranges for the 2-D dc-sweep required to capture the dependence of the stage's output current on its input and output voltages.

Each stage is set to its input and output dc-operating points, and a 2-D dc-sweep of its output current is preformed under no load; the two sweeping parameters are the input and output voltages, with r_1 and r_2 number of steps, respectively.

C. Model Coefficients Extraction via Linear Regression

After all 2-D dc-sweeps are completed, the acquired data have to be processed in an appropriate way to derive each stage's $g_{itj}^{k\ell}$-coefficients. A linear regression approach is used, in the form of a linear least-squares problem [36]

$$I_g = UG + I_\varepsilon. \tag{10}$$

The matrices $U \in \mathbb{R}^{(r_1 \cdot r_2)\times 9}$ and $G \in \mathbb{R}^{9\times 1}$ are defined as

$$U = \left[\widetilde{u}_{itj},\ \widetilde{u}_{itj}^2,\ \widetilde{u}_{itj}^3,\ u_j,\ u_j^2,\ u_j^3,\ \widetilde{u}_{itj}u_j,\ \widetilde{u}_{itj}^2 u_j,\ \widetilde{u}_{itj}u_j^2\right] \tag{11}$$

$$G = \left[g_{itj}^{10},\ g_{itj}^{20},\ g_{itj}^{30},\ g_{itj}^{01},\ g_{itj}^{02},\ g_{itj}^{03},\ g_{itj}^{11},\ g_{itj}^{21},\ g_{itj}^{12}\right]^{\mathrm{T}} \tag{12}$$

forming (8) for all the values of the stage's output current, embodied in $I_g \in \mathbb{R}^{(r_1 \cdot r_2)\times 1}$. The column matrix $I_\varepsilon \in \mathbb{R}^{(r_1 \cdot r_2)\times 1}$ accounts for the error between the current values obtained by simulation (I_g) and the ones resulting from UG.

For normalization purposes, and to ensure a robust solution, a scaling is introduced in (10) by means of a diagonal matrix, D

$$I_g = UD^{-1}DG + I_\varepsilon \tag{13}$$

$$D = \mathrm{diag}(\delta_1, \ldots, \delta_9) \in \mathbb{R}^{9\times 9} \tag{14}$$

where δ_i is the Euclidean norm [37] of the ith column of U. The solution yielding the estimation of the $g_{itj}^{k\ell}$-coefficients is

$$G = D^{-1}\left[\left(UD^{-1}\right)^{\mathrm{T}} UD^{-1}\right]^{-1}\left(UD^{-1}\right)^{\mathrm{T}} I_g. \tag{15}$$

D. Weakly Nonlinear G_m-Stage Behavior Criteria

Although it is not always trivial to confirm that a circuit operates under weak nonlinearities *a priori* [8], it is possible to practically confirm such an operation, subjected to certain bounds. Useful insight can be gained by the following two criteria.

1) Criterion 1: First, the accuracy of the least-squares fit to the simulation current values of a G_m-stage is evaluated by the bounded ratio

$$\frac{\|I_\varepsilon\|_1}{\|I_g\|_1} = \frac{\|I_g - UG\|_1}{\|I_g\|_1} \le b_I \tag{16}$$

where $\|\cdot\|_1$ denotes the 1-norm [37], and $b_I > 0$.

This ratio must be small in order to confirm a good fit. As such, the value of b_I can be adjusted to meet the desired level of accuracy. In the example cases of Section V, a value of b_I in the order of 10^{-4} was found to yield accurate fitting.

2) Criterion 2: After a fit with good accuracy is confirmed, the normalized magnitudes of the nonlinear terms of (8) are considered. Let

$$E\left(\widetilde{u}_{itj}, u_j\right) = \begin{bmatrix} \left|g_{itj}^{10}\widetilde{u}_{itj}\right| & \left|g_{itj}^{20}\widetilde{u}_{itj}^2\right| & \left|g_{itj}^{30}\widetilde{u}_{itj}^3\right| \\ \left|g_{itj}^{01}u_j\right| & \left|g_{itj}^{02}u_j^2\right| & \left|g_{itj}^{03}u_j^3\right| \\ \left|g_{itj}^{11}\widetilde{u}_{itj}u_j\right| & \left|g_{itj}^{21}\widetilde{u}_{itj}^2 u_j\right| & \left|g_{itj}^{12}\widetilde{u}_{itj}u_j^2\right| \end{bmatrix} \in \mathbb{R}^{3\times 3} \tag{17}$$

$$\overline{E} = \frac{1}{\left|g_{itj}^{10}\widetilde{u}_{itj}^{\max}\right|} E\left(\widetilde{u}_{itj}^{\max}, u_j^{\max}\right) \in \mathbb{R}^{3\times 3} \tag{18}$$

where it is assumed that the dominant linear term of (8) is $g_{itj}^{10}\widetilde{u}_{itj}$, and the maximum values $\widetilde{u}_{itj}^{\max}$ and $u_j^{\max}$ are taken from the 2-D dc-sweep ranges of the G_m-stage.

The entries of $\overline{E}$ that correspond to the normalized nonlinear terms of (8) can be bounded by $b_g^{n\ell} > 0$, to ensure that the dominant linear term, $g_{itj}^{10}\widetilde{u}_{itj}$, is at least $1/b_g^{n\ell}$ times stronger over the entire input and output voltage ranges. A value of $b_g^{n\ell}$ in the order of 10^{-1} was found to be reasonable, especially for a stage where $u_j^{\max} \gg \widetilde{u}_{itj}^{\max}$.

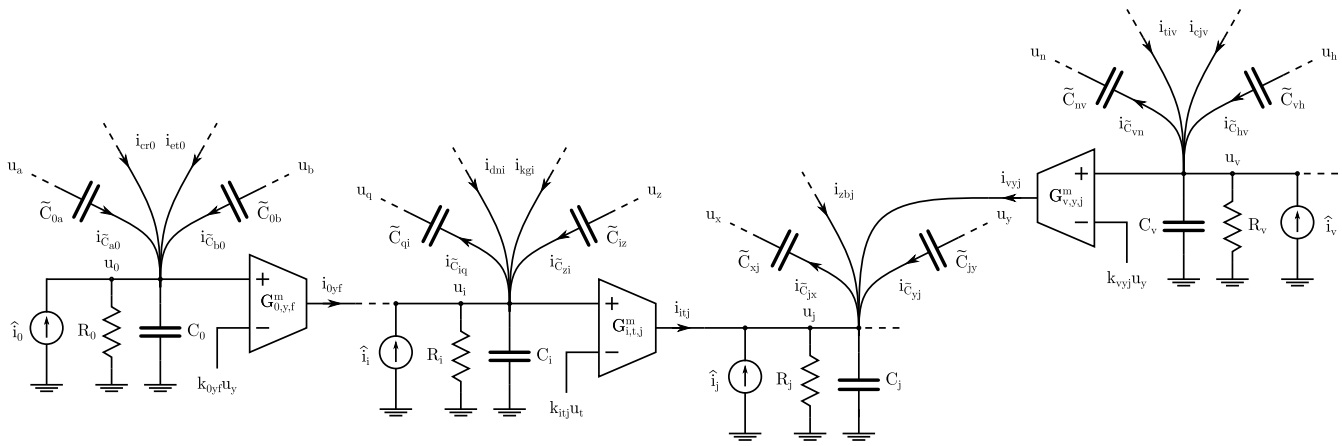

Fig. 14. General circuit structure, composed of G_m-stages.

IV. Harmonic Distortion Estimation

Consider the general circuit structure of Fig. 14. The topology is composed of G_m-stages, resistors and capacitors. Each node $j, j = 0, 1, \ldots, n$, may feature a resistor, R_j, and a capacitor, C_j, connected to ground. It can also have an excitation signal, as an independent current source, $\hat{i}_j$. The G_m-stages behave as described in Section II, while capacitor $\widetilde{C}_{\ell j}$ provides coupling between nodes ℓ and j, with

$$i_{\widetilde{C}_{\ell j}} = \widetilde{C}_{\ell j}(\dot{u}_\ell - \dot{u}_j) = -i_{\widetilde{C}_{j\ell}}. \tag{19}$$

For each node j, it holds

$$\hat{i}_j + \sum_{i,t} i_{itj} + \sum_{\ell} i_{\widetilde{C}_{\ell j}} = \frac{u_j}{R_j} + C_j \dot{u}_j \tag{20}$$

and by using (19)

$$\hat{i}_j + \sum_{i,t} i_{itj} + \sum_{\ell} \widetilde{C}_{\ell j} \dot{u}_\ell = \frac{u_j}{R_j} + \left(C_j + \sum_{\ell} \widetilde{C}_{\ell j} \right) \dot{u}_j. \tag{21}$$

Equation (21) constitutes a manipulated form of the state-space equation of the general form $C^c \dot{u} = G^c u + \hat{I}$, where C^c and G^c are the corresponding capacitance and conductance matrices of the whole circuit.

Assuming that the circuit operates in steady-state, let the voltage of node j be of the form (recall that only harmonics up to the third are considered)

$$u_j = u_j^f + u_j^h \tag{22}$$

$$u_j^f = \theta^f S_j^f \tag{22a}$$

$$u_j^h = \theta^h S_j^h \tag{22b}$$

where[5]

$$S_j^f = \left[a_{j,1}, \quad b_{j,1}\right]^{\mathrm{T}} \in \mathbb{R}^{2\times 1} \tag{23}$$

$$S_j^h = \left[a_{j,2}, \quad b_{j,2}, \quad a_{j,3}, \quad b_{j,3}\right]^{\mathrm{T}} \in \mathbb{R}^{4\times 1} \tag{24}$$

$$\theta^f = \left[\sin \omega t, \quad \cos \omega t\right] \in \mathbb{R}^{1\times 2} \tag{25}$$

$$\theta^h = \left[\sin 2\omega t, \quad \cos 2\omega t, \quad \sin 3\omega t, \quad \cos 3\omega t\right] \in \mathbb{R}^{1\times 4}. \tag{26}$$

[5]Vectors θ^f and θ^h are functions of time, so a more appropriate notation would be that of $\theta^f(t)$ and $\theta^h(t)$; time is omitted for simplicity.

Terms u_j^f and u_j^h represent the voltage components of the fundamental and the harmonic tones, respectively, while vectors S_j^f and S_j^h feature the corresponding sin and cos coefficients.

In the same vein, for the excitation current source of node j it is

$$\hat{i}_j = \hat{i}_j^f + \hat{i}_j^h \tag{27}$$

$$\hat{i}_j^f = \theta^f P_j^f \tag{27a}$$

$$\hat{i}_j^h = \theta^h P_j^h \tag{27b}$$

where

$$P_j^f = \left[\hat{a}_{j,1}, \quad \hat{b}_{j,1}\right]^{\mathrm{T}} \in \mathbb{R}^{2\times 1} \tag{28}$$

$$P_j^h = \left[\hat{a}_{j,2}, \quad \hat{b}_{j,2}, \quad \hat{a}_{j,3}, \quad \hat{b}_{j,3}\right]^{\mathrm{T}} \in \mathbb{R}^{4\times 1}. \tag{29}$$

In the following analysis, it has been assumed that the circuit features only one excitation source, that of node 0.

The proposed harmonic distortion estimation method is performed in two steps. First, the fundamental tone of ω is estimated, followed by the estimation of the harmonic tones of 2ω and 3ω, to finally derive HD_2 and HD_3.

A. Fundamental Tone Estimation

Since weak nonlinearities are assumed, their contribution to the fundamental tone can be considered negligible. Thus, the fundamental tone voltage component of node j, (22a), should satisfy the linear part of (21). As such, for the fundamental tone estimation, the output current, i_{itj}^f, of stage $G_{i,t,j}^m$, is expressed using (3) and (22a) as only the linear part of (8)

$$i_{itj}^f = \theta^f \left(g_{itj}^{10} S_i^f - g_{itj}^{10} k_{itj} S_t^f + g_{itj}^{01} S_j^f \right). \tag{30}$$

That is, a G_m-stage's output current is the sum of three independent ones, each one linearly dependent on the fundamental tone voltage component of its corresponding node.

The expression of i_{itj}^f can be used to form a system of equations for the fundamental tone coefficients of the complete circuit under consideration, relying on (21). Let

$$J = \begin{bmatrix} 0 & -1 \\ 1 & 0 \end{bmatrix} \in \mathbb{R}^{2\times 2}. \tag{31}$$

Then, it is

$$\dot{u}_j^f = \dot{\theta}^f S_j^f = \omega\theta^f J S_j^f. \tag{32}$$

Combining (30) and (32) with (21) results in

$$\theta^f\left[P_j^f + \sum_{i,t}\left(g_{itj}^{10}S_i^f - g_{itj}^{10}k_{itj}S_t^f + g_{itj}^{01}S_j^f\right) + \sum_{\ell}\widetilde{C}_{\ell j}\omega J S_\ell^f\right] = \theta^f\left[\frac{1}{R_j}S_j^f + \left(C_j + \sum_{\ell}\widetilde{C}_{\ell j}\right)\omega J S_j^f\right]. \tag{33}$$

The vector function θ^f consists of two linearly independent functions of time, and embodies two independent equations with respect to the coefficients of $\sin\omega t$ and $\cos\omega t$. So, θ^f can be eliminated for (33) to hold for any $t \in \mathbb{R}$. Reordering terms yields

$$P_j^f + \sum_{i,t} g_{itj}^{10}S_i^f - \sum_{i,t} g_{itj}^{10}k_{itj}S_t^f + \omega\sum_{\ell}\widetilde{C}_{\ell j}JS_\ell^f = \left(\frac{1}{R_j} - \sum_{i,t} g_{itj}^{01}\right)S_j^f + \omega\left(C_j + \sum_{\ell}\widetilde{C}_{\ell j}\right)JS_j^f. \tag{34}$$

Consider the vector of the fundamental tone coefficients of all voltages

$$S^f = \left[\left(S_0^f\right)^{\mathrm{T}},\quad \left(S_1^f\right)^{\mathrm{T}},\quad \ldots,\quad \left(S_n^f\right)^{\mathrm{T}}\right]^{\mathrm{T}} \in \mathbb{R}^{2(n+1)\times 1} \tag{35}$$

and that of the excitation current source[6]

$$P^f = \left[\left(P_0^f\right)^{\mathrm{T}},\quad \left(0,\ 0\right),\quad \ldots,\quad \left(0,\ 0\right)\right]^{\mathrm{T}} \in \mathbb{R}^{2(n+1)\times 1}. \tag{36}$$

Then, the equivalent of (34) for the whole circuit structure is constructed in a block-matrix form

$$P^f + \left(G^f + K^f + \omega F^f\right)S^f = \left(T^f + \omega W^f\right)S^f \tag{37}$$

where

$$G^f = \left[\sum_t g_{itj}^{10}\right]_{j,i=0}^{n} \otimes I_2 \in \mathbb{R}^{2(n+1)\times 2(n+1)} \tag{38}$$

$$K^f = \left[-\sum_i g_{itj}^{10}k_{itj}\right]_{j,t=0}^{n} \otimes I_2 \in \mathbb{R}^{2(n+1)\times 2(n+1)} \tag{39}$$

$$F^f = \left[\widetilde{C}_{\ell j}\right]_{j,\ell=0}^{n} \otimes J \in \mathbb{R}^{2(n+1)\times 2(n+1)} \tag{40}$$

$$T^f = \mathrm{diag}\left(\left[\frac{1}{R_j} - \sum_{i,t} g_{itj}^{01}\right]_{j=0}^{n}\right) \otimes I_2 \in \mathbb{R}^{2(n+1)\times 2(n+1)} \tag{41}$$

$$W^f = \mathrm{diag}\left(\left[C_j + \sum_{\ell}\widetilde{C}_{\ell j}\right]_{j=0}^{n}\right) \otimes J \in \mathbb{R}^{2(n+1)\times 2(n+1)}. \tag{42}$$

In (38)–(42), $\otimes$ denotes the Kronecker's product [37], and I_n is the $n \times n$ identity matrix. The vector of the fundamental tone coefficients is the solution of (37)

$$S^f = \left[T^f - G^f - K^f + \omega\left(W^f - F^f\right)\right]^{-1}P^f. \tag{43}$$

[6]If more than one excitation signals are present, they should be included in the corresponding entries of the vector.

B. Harmonic Tones Estimation

The harmonic tones voltage components of node j, (22b), are generated by the nonlinear terms of (8). Including all voltage terms in the form of (22) and computing all produced terms would result in cumbersome expressions that constitute a nonlinear equality problem. Even though this approach yields the exact algebraic solution, it is neither easy to implement nor computationally efficient.

A close inspection of (8), in association with (22), reveals that the generated coefficients of the second and third harmonic tones due to the nonlinear terms of (8) will eventually be a sum of products of the following.

a) Only fundamental tone coefficients.
b) A single harmonic tone coefficient to the power of one and one or more fundamental tone coefficients.
c) Higher orders or products of harmonic tones coefficients.

Since the amplitudes of the harmonic tones are expected to be much smaller than that of the fundamental tone, products involving two or more harmonic tones coefficients or powers of them are negligible and can be safely ignored. This approximation can be validated after the estimation of the harmonic tones, as demonstrated in Section IV-C.

Based on the above and including the linear part of (8), the output current, i_{itj}^h, of stage $G_{i,t,j}^m$, can be approximated, using (3) and (22b), by

$$i_{itj}^h = \theta^h\Big[g_{itj}^{10}S_i^h - g_{itj}^{10}k_{itj}S_t^h + g_{itj}^{01}S_j^h + Z_{itj} + X_{itj}^{\alpha}S_i^h + X_{itj}^{\beta}S_t^h + X_{itj}^{\gamma}S_j^h\Big] \tag{44}$$

where the term $\theta^h Z_{itj}$ is the sum of the products a), and the term $\theta^h(X_{itj}^{\alpha}S_i^h + X_{itj}^{\beta}S_t^h + X_{itj}^{\gamma}S_j^h)$ is the sum of the products b). Note that the approximate expression of i_{itj}^h is linear to the corresponding harmonic tones coefficients.

The term Z_{itj} is expressed as

$$Z_{itj} = \left[p_{itj}^{s2},\quad p_{itj}^{c2},\quad p_{itj}^{s3},\quad p_{itj}^{c3}\right]^{\mathrm{T}} \in \mathbb{R}^{4\times 1} \tag{45}$$

where

$$p_{itj}^{s2} = g_{itj}^{20}\widetilde{f}_{itj}^{s2} + g_{itj}^{02}f_j^{s2} + g_{itj}^{11}h_{itj}^{s2} \tag{46}$$

$$p_{itj}^{c2} = g_{itj}^{20}\widetilde{f}_{itj}^{c2} + g_{itj}^{02}f_j^{c2} + g_{itj}^{11}h_{itj}^{c2} \tag{47}$$

$$p_{itj}^{s3} = g_{itj}^{30}\widetilde{f}_{itj}^{s3} + g_{itj}^{03}f_j^{s3} + g_{itj}^{21}r_{iij}^{s3} + g_{itj}^{12}o_{itj}^{s3} \tag{48}$$

$$p_{itj}^{c3} = g_{itj}^{30}\widetilde{f}_{itj}^{c3} + g_{itj}^{03}f_j^{c3} + g_{itj}^{21}r_{itj}^{c3} + g_{itj}^{12}o_{itj}^{c3}. \tag{49}$$

Furthermore, matrices $X_{itj}^{\alpha} \in \mathbb{R}^{4\times 4}$, $X_{itj}^{\beta} \in \mathbb{R}^{4\times 4}$, and $X_{itj}^{\gamma} \in \mathbb{R}^{4\times 4}$ are defined as

$$X_{itj}^{\alpha} = g_{itj}^{20}\widetilde{N}_{itj} + g_{itj}^{30}\frac{3}{2}\widetilde{M}_{itj} + g_{itj}^{11}\frac{1}{2}N_j + g_{itj}^{21}Q_{itj} + g_{itj}^{12}\frac{1}{2}M_j \tag{50}$$

$$X_{itj}^{\beta} = -k_{itj}X_{itj}^{\alpha} \tag{51}$$

$$X_{itj}^{\gamma} = g_{itj}^{02}N_j + g_{itj}^{03}\frac{3}{2}M_j + g_{itj}^{11}\frac{1}{2}\widetilde{N}_{itj} + g_{itj}^{21}\frac{1}{2}\widetilde{M}_{itj} + g_{itj}^{12}Q_{itj}. \tag{52}$$

The quantities forming (46)–(52) can be found in the Appendix and are omitted from this part of the text for better comprehension of the method's steps.

Expression (44) is now used to form a system of equations for the harmonic tones coefficients, based again on (21). To

this end, let

$$L = \begin{bmatrix} 2 & 0 \\ 0 & 3 \end{bmatrix} \in \mathbb{R}^{2\times 2} \tag{53}$$

and express

$$\dot{u}_j^h = \dot{\theta}^h S_j^h = \omega\theta^h (L \otimes J) S_j^h. \tag{54}$$

The combination of (44) and (54) with (21) yields

$$\begin{aligned}\theta^h \Bigg[& P_j^h + \sum_{i,t}\Big(g_{itj}^{10} S_i^h - g_{itj}^{10} k_{itj} S_t^h + g_{itj}^{01} S_j^h + Z_{itj} \\ & + X_{itj}^{\alpha} S_i^h + X_{itj}^{\beta} S_t^h + X_{itj}^{\gamma} S_j^h \Big) + \sum_{\ell} \widetilde{C}_{\ell j} \omega (L \otimes J) S_\ell^h \Bigg] \\ = \theta^h \Bigg[& \frac{1}{R_j} S_j^h + \Bigg(C_j + \sum_{\ell} \widetilde{C}_{\ell j} \Bigg) \omega (L \otimes J) S_j^h \Bigg]. \end{aligned} \tag{55}$$

The vector function θ^h consists of four linearly independent functions of time, implying four equations of the coefficients of $\sin 2\omega t$, $\cos 2\omega t$, $\sin 3\omega t$, and $\cos 3\omega t$. Eliminating θ^h and reordering terms results in

$$\begin{aligned} & \Bigg(P_j^h + \sum_{i,t} Z_{itj} \Bigg) + \sum_{i,t} g_{itj}^{10} S_i^h - \sum_{i,t} g_{itj}^{10} k_{itj} S_t^h \\ & + \sum_{i,t}\Big(X_{itj}^{\alpha} S_i^h + X_{itj}^{\beta} S_t^h + X_{itj}^{\gamma} S_j^h \Big) + \omega \sum_{\ell} \widetilde{C}_{\ell j} (L \otimes J) S_\ell^h \\ & = \Bigg(\frac{1}{R_j} - \sum_{i,t} g_{itj}^{01} \Bigg) S_j^h + \omega \Bigg(C_j + \sum_{\ell} \widetilde{C}_{\ell j} \Bigg) (L \otimes J) S_j^h. \end{aligned} \tag{56}$$

Let the vector of the harmonic tones coefficients of all voltages of the circuit be

$$S^h = \Big[\big(S_0^h\big)^{\mathrm{T}}, \quad \big(S_1^h\big)^{\mathrm{T}}, \quad \ldots, \quad \big(S_n^h\big)^{\mathrm{T}} \Big]^{\mathrm{T}} \in \mathbb{R}^{2(n+1)\times 1} \tag{57}$$

and consider the vector $P^h \in \mathbb{R}^{4(n+1)\times 1}$ of the excitation current source[7]

$$P^h = \Big[\big(P_0^h\big)^{\mathrm{T}}, \quad \big(0,\ 0,\ 0,\ 0\big), \quad \ldots, \quad \big(0,\ 0,\ 0,\ 0\big) \Big]^{\mathrm{T}}. \tag{58}$$

Moreover, let the vector

$$B^h = P^h + Z^h \in \mathbb{R}^{4(n+1)\times 1} \tag{59}$$

where

$$Z^h = \big[\textstyle\sum_{i,t} Z_{itj} \big]_{j=0}^{n} \in \mathbb{R}^{4(n+1)\times 1}. \tag{60}$$

Then, (56) is written in block-matrix form

$$B^h + \Big(G^h + K^h + X^h + \omega F^h \Big) S^h = \Big(T^h + \omega W^h \Big) S^h \tag{61}$$

[7]In the case of more than one excitation signals being present, they should be added at the corresponding entries of the vector.

where

$$G^h = G^f \otimes I_2 \in \mathbb{R}^{4(n+1)\times 4(n+1)} \tag{62}$$

$$K^h = K^f \otimes I_2 \in \mathbb{R}^{4(n+1)\times 4(n+1)} \tag{63}$$

$$F^h = \big[\widetilde{C}_{\ell j} \big]_{j,\ell=0}^{n} \otimes (L \otimes J) \in \mathbb{R}^{4(n+1)\times 4(n+1)} \tag{64}$$

$$T^h = T^f \otimes I_2 \in \mathbb{R}^{4(n+1)\times 4(n+1)} \tag{65}$$

$$W^h = \mathrm{diag}\Big(\big[C_j + \textstyle\sum_{\ell} \widetilde{C}_{\ell j} \big]_{j=0}^{n} \Big) \otimes (L \otimes J) \in \mathbb{R}^{4(n+1)\times 4(n+1)} \tag{66}$$

$$\begin{aligned} X^h = & \Big[\textstyle\sum_t X_{itj}^{\alpha} \Big]_{j,i=0}^{n} + \Big[\textstyle\sum_i X_{itj}^{\beta} \Big]_{j,t=0}^{n} \\ & + \bigoplus_{j=0}^{n} \Big[\textstyle\sum_{i,t} X_{itj}^{\gamma} \Big] \in \mathbb{R}^{4(n+1)\times 4(n+1)} \end{aligned} \tag{67}$$

and $\bigoplus$ denotes the direct sum of matrices [38].

The solution of (61) gives the vector of the harmonic tones coefficients

$$S^h = \Big[T^h - G^h - K^h - X^h + \omega \Big(W^h - F^h \Big) \Big]^{-1} B^h. \tag{68}$$

The solution of (43) and (68) can be easily calculated, making the speed and computational efficiency of the proposed method superior to that of traditional distortion estimation via simulation.

Since all coefficients are known, the desired HD_2 and HD_3 factors can be immediately obtained for any node j of the circuit

$$\mathrm{HD}_2^j = 10 \log_{10} \left(\frac{a_{j,2}^2 + b_{j,2}^2}{a_{j,1}^2 + b_{j,1}^2} \right) \tag{69}$$

$$\mathrm{HD}_3^j = 10 \log_{10} \left(\frac{a_{j,3}^2 + b_{j,3}^2}{a_{j,1}^2 + b_{j,1}^2} \right). \tag{70}$$

For a differential output, between nodes j and m, the distortion factors are given by

$$\mathrm{HD}_2^{jm} = 10 \log_{10} \left[\frac{\big(a_{j,2} - a_{m,2}\big)^2 + \big(b_{j,2} - b_{m,2}\big)^2}{\big(a_{j,1} - a_{m,1}\big)^2 + \big(b_{j,1} - b_{m,1}\big)^2} \right] \tag{71}$$

$$\mathrm{HD}_3^{jm} = 10 \log_{10} \left[\frac{\big(a_{j,3} - a_{m,3}\big)^2 + \big(b_{j,3} - b_{m,3}\big)^2}{\big(a_{j,1} - a_{m,1}\big)^2 + \big(b_{j,1} - b_{m,1}\big)^2} \right]. \tag{72}$$

C. Harmonic Tones Approximation Error Evaluation

The assumption regarding the amplitudes of the harmonic tones that led to the elimination of the products c) in Section IV-B can be validated retrospectively after the solution of (43) and (68). To this end, consider the error excitation current source of stage $G_{i,t,j}^m$

$$\hat{i}_{itj}^{\varepsilon} = \theta^h \hat{P}_{itj}^{\varepsilon} = \theta^h \big[\hat{a}_{itj,2}^{\varepsilon}, \quad 0, \quad \hat{a}_{itj,3}^{\varepsilon}, \quad 0 \big]^{\mathrm{T}} \tag{73}$$

where $\hat{P}_{itj}^{\varepsilon} \in \mathbb{R}^{4\times 1}$ has the same form as (29) and

$$\begin{aligned} \hat{a}_{itj,2}^{\varepsilon} = & \Big| g_{itj}^{30} \Big| \left(\frac{3}{2} \widetilde{c}_{itj} \widetilde{d}_{itj}^2 + \frac{9}{4} \widetilde{d}_{itj}^3 \right) + \Big| g_{itj}^{03} \Big| \left(\frac{3}{2} c_j d_j^2 + \frac{9}{4} d_j^3 \right) \\ & + \Big| g_{itj}^{21} \Big| \left(\frac{1}{2} c_j \widetilde{d}_{itj}^2 + \widetilde{c}_{itj} \widetilde{d}_{itj} d_j + \frac{9}{4} \widetilde{d}_{itj}^2 d_j \right) \\ & + \Big| g_{itj}^{12} \Big| \left(\frac{1}{2} \widetilde{c}_{itj} d_j^2 + c_j \widetilde{d}_{itj} d_j + \frac{9}{4} \widetilde{d}_{itj} d_j^2 \right) \end{aligned} \tag{74}$$

$$\hat{a}^{\varepsilon}_{itj,3} = \left|g^{30}_{itj}\right|\left(\frac{3}{4}\widetilde{c}_{itj}\widetilde{d}^2_{itj} + \frac{9}{4}\widetilde{d}^3_{itj}\right) + \left|g^{03}_{itj}\right|\left(\frac{3}{4}c_j d_j^2 + \frac{9}{4}d_j^3\right) + \left|g^{21}_{itj}\right|\left(\frac{1}{4}c_j\widetilde{d}^2_{itj} + \frac{1}{2}\widetilde{c}_{itj}\widetilde{d}_{itj}d_j + \frac{9}{4}\widetilde{d}^2_{itj}d_j\right) + \left|g^{12}_{itj}\right|\left(\frac{1}{4}\widetilde{c}_{itj}d_j^2 + \frac{1}{2}c_j\widetilde{d}_{itj}d_j + \frac{9}{4}\widetilde{d}_{itj}d_j^2\right). \quad (75)$$

The coefficients involved in (74) and (75) are the maximum amplitude values of the fundamental and any harmonic tone at the input and the output of stage $G^m_{i,t,j}$, over the entire frequency range of interest, evaluated as

$$\widetilde{c}_{itj} = \max\left\{\sqrt{\widetilde{a}^2_{itj,1} + \widetilde{b}^2_{itj,1}}\right\} \quad (76)$$

$$c_j = \max\left\{\sqrt{a^2_{j,1} + b^2_{j,1}}\right\} \quad (77)$$

$$\widetilde{d}_{itj} = \max\left\{\sqrt{\widetilde{a}^2_{itj,2} + \widetilde{b}^2_{itj,2}}, \sqrt{\widetilde{a}^2_{itj,3} + \widetilde{b}^2_{itj,3}}\right\} \quad (78)$$

$$d_j = \max\left\{\sqrt{a^2_{j,2} + b^2_{j,2}}, \sqrt{a^2_{j,3} + b^2_{j,3}}\right\} \quad (79)$$

where

$$\widetilde{a}_{itj,1} = a_{i,1} - k_{itj}a_{t,1} \quad (80)$$

$$\widetilde{b}_{itj,1} = b_{i,1} - k_{itj}b_{t,1} \quad (81)$$

$$\widetilde{a}_{itj,2} = a_{i,2} - k_{itj}a_{t,2} \quad (82)$$

$$\widetilde{b}_{itj,2} = b_{i,2} - k_{itj}b_{t,2} \quad (83)$$

$$\widetilde{a}_{itj,3} = a_{i,3} - k_{itj}a_{t,3} \quad (84)$$

$$\widetilde{b}_{itj,3} = b_{i,3} - k_{itj}b_{t,3}. \quad (85)$$

The current of (73) is injected into the output node, j, of stage $G^m_{i,t,j}$, while no other input is present in the circuit under consideration. The expression of $\hat{i}^{\varepsilon}_{itj}$ accounts for the products c) that would have been generated by the nonlinear terms of (8). Its magnitude is an overestimation of the induced error in the estimation of the harmonic tones by (68); the maximum values of (76)–(79) may not be an input-output corresponding pair in frequency, and may also result from a combination of both harmonic tones. Furthermore, the involved $g^{k\ell}_{itj}$-coefficients are summed in absolute-value fashion, while they may feature opposite signs.

The harmonic tones coefficients due to the error current source of stage $G^m_{i,t,j}$ are given by the solution of

$$S^{h,\varepsilon}_{itj} = \left[T^h - G^h - K^h + \omega\left(W^h - F^h\right)\right]^{-1} P^{h,\varepsilon}_{itj} \quad (86)$$

where

$$P^{h,\varepsilon}_{itj} = \Big[\left(0,\ 0,\ 0,\ 0\right),\ \ldots,\ \overbrace{\left(\hat{a}^{\varepsilon}_{itj,2},\ 0,\ \hat{a}^{\varepsilon}_{itj,3},\ 0\right)}^{\text{node } j},\ \ldots,\ \left(0,\ 0,\ 0,\ 0\right)\Big]^{\mathrm{T}} \in \mathbb{R}^{4(n+1)\times 1}. \quad (87)$$

This procedure is repeated for all G_m-stages of the circuit, and a total error estimation is obtained by summing the absolute coefficient values of all $S^{h,\varepsilon}_{itj} \in \mathbb{R}^{4(n+1)\times 1}$ vectors

$$S^{h,\varepsilon} = \sum_{itj}\Big[\left|a^{\varepsilon}_{0,2}\right|,\ \left|b^{\varepsilon}_{0,2}\right|,\ \left|a^{\varepsilon}_{0,3}\right|,\ \left|b^{\varepsilon}_{0,3}\right|\ \left|a^{\varepsilon}_{1,2}\right|,\ \left|b^{\varepsilon}_{1,2}\right|,\ \left|a^{\varepsilon}_{1,3}\right|,\ \left|b^{\varepsilon}_{1,3}\right|\ \ldots,\ \left|a^{\varepsilon}_{n,2}\right|,\ \left|b^{\varepsilon}_{n,2}\right|,\ \left|a^{\varepsilon}_{n,3}\right|,\ \left|b^{\varepsilon}_{n,3}\right|\Big]^{\mathrm{T}} \in \mathbb{R}^{4(n+1)\times 1}. \quad (88)$$

Procedure 1: Proposed Harmonic Distortion Estimation Method

1: Decompose the circuit as an interconnection of CMOS stages.
2: Derive each stage's $g^{k\ell}_{itj}$-coefficients by curve-fitting, confirming the criteria of Section III-D1 and Section III-D2.
3: Replace each CMOS stage with its G_m-stage model equivalent.
4: Add all resistors and capacitors, including parasitic ones if of interest.
5: Add the circuit's excitation current source(s).
6: Form matrices (36), (38)–(42) and solve (43) for the fundamental tone estimation.
7: Form matrices (58)–(60), (62)–(67) and solve (68) for the harmonic tones estimation, evaluating the harmonic tones approximation of Section IV-B with the procedure of Section IV-C.
8: Use (69), (70) or (71), (72) to estimate the desired HD_2 and HD_3 factors.

Again, this constitutes an overestimation of the total propagated error, since (88) supposes all calculated coefficients to be in phase at every node of the circuit.

The final step to validate the harmonic tones approximation is to compare the power of the second and the third harmonic estimated by (68) to the power of the ones resulting from (88), in the frequency range of interest. The power difference would indicate a pessimistic error estimation in the second and the third harmonic, and thus in HD_2 and HD_3 factors.

D. Proposed Method Application Procedure

Concluding the theoretical analysis of the harmonic distortion estimation, the application of the proposed method is summarized as Procedure 1.

E. Application Examples

The application of the proposed method is illustrated via two example cases, where the necessary parameters are derived and all calculation steps are followed. The examples are continued in Section V, where the estimated distortion factors are compared to that resulting by simulation, for a range of frequencies.

1) One-Stage Cascode Amplifier: Consider the one-stage cascode amplifier of Fig. 15. The load, $R_L \| C_L$, is connected to ground via a dc-voltage of V^{op}_{OUT}, equal to the dc-voltage of the unloaded output of the amplifier.

The equivalent G_m-stage representation is shown in Fig. 16, where the whole stage is treated as a single G_m-stage, $G^m_{0,r,1}$. The ac-input signal, $u_{in} = u_0$, is realized by $\hat{i}_0 = u_0/R_0$ acting on $R_0 = 1\ \Omega$, and $R_L = R_1$, $C_L = C_1$.

Given the stage's derived $g^{k\ell}_{0r1}$-coefficients, the necessary matrices are defined according to (35), (36), and (38)–(42)

$$S^f = \left[a_{0,1},\quad b_{0,1},\quad a_{1,1},\quad b_{1,1}\right]^{\mathrm{T}}$$

$$P^f = \left[\hat{a}_{0,1},\quad \hat{b}_{0,1},\quad 0,\quad 0\right]^{\mathrm{T}}$$

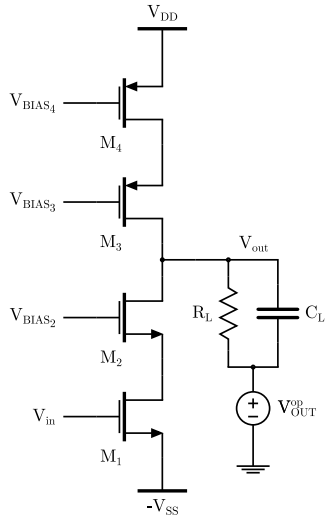

Fig. 15. One-stage cascode amplifier.

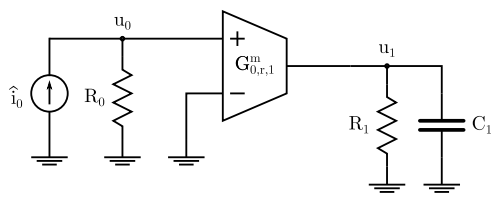

Fig. 16. G_m-stage equivalent representation of the one-stage cascode amplifier.

and

$$G^f = \begin{bmatrix} 0 & 0 \\ g^{10}_{0r1} & 0 \end{bmatrix} \otimes I_2$$
$$K^f = 0_4$$
$$F^f = 0_4$$
$$T^f = \begin{bmatrix} \frac{1}{R_0} & 0 \\ 0 & \frac{1}{R_1} - g^{01}_{0r1} \end{bmatrix} \otimes I_2$$
$$W^f = \begin{bmatrix} 0 & 0 \\ 0 & C_1 \end{bmatrix} \otimes J$$

where 0_n denotes the $n \times n$ zero matrix. Then, the solution for the fundamental tone coefficients comes directly from (43).

The harmonic tones coefficients vector, S^h, and the vector B^h are defined according to (57)–(60)

$$S^h = \left[a_{0,2},\ b_{0,2},\ a_{0,3},\ b_{0,3},\ a_{1,2},\ b_{1,2},\ a_{1,3},\ b_{1,3}\right]^{\mathrm{T}}$$
$$B^h = \left[\hat{a}_{0,2},\ \hat{b}_{0,2},\ \hat{a}_{0,3},\ \hat{b}_{0,3},\ p^{s2}_{0r1},\ p^{c2}_{0r1},\ p^{s3}_{0r1},\ p^{c3}_{0r1}\right]^{\mathrm{T}}$$

where the following are calculated using (46)–(49)

$$p^{s2}_{0r1} = g^{20}_{0r1}\widetilde{f}^{s2}_{0r1} + g^{02}_{0r1}f^{s2}_1 + g^{11}_{0r1}h^{s2}_{0r1}$$
$$p^{c2}_{0r1} = g^{20}_{0r1}\widetilde{f}^{c2}_{0r1} + g^{02}_{0r1}f^{c2}_1 + g^{11}_{0r1}h^{c2}_{0r1}$$
$$p^{s3}_{0r1} = g^{30}_{0r1}\widetilde{f}^{s3}_{0r1} + g^{03}_{0r1}f^{s3}_1 + g^{21}_{0r1}r^{s3}_{0r1} + g^{12}_{0r1}o^{s3}_{0r1}$$
$$p^{c3}_{0r1} = g^{30}_{0r1}\widetilde{f}^{c3}_{0r1} + g^{03}_{0r1}f^{c3}_1 + g^{21}_{0r1}r^{c3}_{0r1} + g^{12}_{0r1}o^{c3}_{0r1}$$

and (89)–(102) are calculated for $\widetilde{a}_{0r1,1} = a_{0,1}$, $\widetilde{b}_{0r1,1} = b_{0,1}$, $a_{1,1}$, and $b_{1,1}$. Finally, following (50)–(52) and (62)–(67), it is

$$G^h = G^f \otimes I_2$$
$$K^h = 0_8$$
$$F^h = 0_8$$
$$T^h = T^f \otimes I_2$$
$$W^h = \begin{bmatrix} 0 & 0 \\ 0 & C_1 \end{bmatrix} \otimes (L \otimes J)$$
$$X^h = \begin{bmatrix} 0_4 & 0_4 \\ X^{\alpha}_{0r1} & X^{\gamma}_{0r1} \end{bmatrix}$$

where

$$X^{\alpha}_{0r1} = g^{20}_{0r1}\widetilde{N}_{0r1} + g^{30}_{0r1}\frac{3}{2}\widetilde{M}_{0r1} + g^{11}_{0r1}\frac{1}{2}N_1 + g^{21}_{0r1}Q_{0r1} + g^{12}_{0r1}\frac{1}{2}M_1$$
$$X^{\gamma}_{0r1} = g^{02}_{0r1}N_1 + g^{03}_{0r1}\frac{3}{2}M_1 + g^{11}_{0r1}\frac{1}{2}\widetilde{N}_{0r1} + g^{21}_{0r1}\frac{1}{2}\widetilde{M}_{0r1} + g^{12}_{0r1}Q_{0r1}$$

and the matrices of (103)–(107) are similarly calculated for $\widetilde{a}_{0r1,1} = a_{0,1}$, $\widetilde{b}_{0r1,1} = b_{0,1}$, $a_{1,1}$, and $b_{1,1}$. The harmonic tones solution is given by (68), enabling the estimation of HD_2 and HD_3 at the amplifier's output.

2) Three-Stage Feedback Amplifier: A more general example is given for the three-stage feedback amplifier of Fig. 9. The application of the method on the equivalent network of Fig. 10 yields the following matrices according to the definitions of (38)–(42)

$$G^f = \begin{bmatrix} 0 & 0 & 0 & 0 & 0 \\ g^{10}_{031} & 0 & 0 & 0 & 0 \\ 0 & g^{10}_{2r1} & 0 & 0 & 0 \\ 0 & 0 & g^{10}_{233} & 0 & 0 \\ 0 & 0 & g^{10}_{244} & 0 & 0 \end{bmatrix} \otimes I_2$$
$$K^f = \begin{bmatrix} 0 & 0 & 0 & 0 & 0 \\ 0 & 0 & 0 & -g^{10}_{031}k_{031} & 0 \\ 0 & 0 & 0 & 0 & 0 \\ 0 & 0 & 0 & -g^{10}_{233} & 0 \\ 0 & 0 & 0 & 0 & -g^{10}_{244} \end{bmatrix} \otimes I_2$$
$$F^f = \begin{bmatrix} 0 & 0 & 0 & 0 & 0 \\ 0 & 0 & 0 & 0 & \widetilde{C}_{14} \\ 0 & 0 & 0 & 0 & 0 \\ 0 & 0 & 0 & 0 & 0 \\ 0 & \widetilde{C}_{14} & 0 & 0 & 0 \end{bmatrix} \otimes J$$
$$T^f = \begin{bmatrix} \frac{1}{R_0} & 0 & 0 & 0 & 0 \\ 0 & -g^{01}_{031} & 0 & 0 & 0 \\ 0 & 0 & -g^{01}_{1r2} & 0 & 0 \\ 0 & 0 & 0 & \frac{1}{R_3} - g^{01}_{233} & 0 \\ 0 & 0 & 0 & 0 & -g^{01}_{244} \end{bmatrix} \otimes I_2$$
$$W^f = \begin{bmatrix} 0 & 0 & 0 & 0 & 0 \\ 0 & \widetilde{C}_{14} & 0 & 0 & 0 \\ 0 & 0 & 0 & 0 & 0 \\ 0 & 0 & 0 & C_3 & 0 \\ 0 & 0 & 0 & 0 & \widetilde{C}_{14} \end{bmatrix} \otimes J.$$

The vectors S^f and P^f of (35) and (36) are omitted for simplicity. Then, (43) gives the fundamental tone coefficients for all nodes of the circuit.

For the harmonic tones estimation, the matrices of (62)–(67) are

$$G^h = G^f \otimes I_2$$
$$K^h = K^f \otimes I_2$$

$$F^h = \begin{bmatrix} 0 & 0 & 0 & 0 & 0 \\ 0 & 0 & 0 & 0 & \widetilde{C}_{14} \\ 0 & 0 & 0 & 0 & 0 \\ 0 & 0 & 0 & 0 & 0 \\ 0 & \widetilde{C}_{14} & 0 & 0 & 0 \end{bmatrix} \otimes (L \otimes J)$$

$$T^h = T^f \otimes I_2$$

$$W^h = \begin{bmatrix} 0 & 0 & 0 & 0 & 0 \\ 0 & \widetilde{C}_{14} & 0 & 0 & 0 \\ 0 & 0 & 0 & 0 & 0 \\ 0 & 0 & 0 & C_3 & 0 \\ 0 & 0 & 0 & 0 & \widetilde{C}_{14} \end{bmatrix} \otimes (L \otimes J)$$

$$X^h = \begin{bmatrix} 0_4 & 0_4 & 0_4 & 0_4 & 0_4 \\ X^{\alpha}_{031} & X^{\gamma}_{031} & 0_4 & X^{\beta}_{031} & 0_4 \\ 0_4 & X^{\alpha}_{1r2} & X^{\gamma}_{1r2} & 0_4 & 0_4 \\ 0_4 & 0_4 & X^{\alpha}_{233} & X^{\beta}_{233} + X^{\gamma}_{233} & 0_4 \\ 0_4 & 0_4 & X^{\alpha}_{244} & 0_4 & X^{\beta}_{244} + X^{\gamma}_{244} \end{bmatrix}$$

where the following are calculated using (50)–(52), the corresponding (80), (81), and (103)–(107)

$$\begin{aligned}
X^{\alpha}_{031} &= g^{20}_{031}\widetilde{N}_{031} + g^{30}_{031}\frac{3}{2}\widetilde{M}_{031} + g^{11}_{031}\frac{1}{2}N_1 + g^{21}_{031}Q_{031} \\
&\quad + g^{12}_{031}\frac{1}{2}M_1 \\
X^{\beta}_{031} &= -k_{031}X^{\alpha}_{031} \\
X^{\gamma}_{031} &= g^{02}_{031}N_1 + g^{03}_{031}\frac{3}{2}M_1 + g^{11}_{031}\frac{1}{2}\widetilde{N}_{031} + g^{21}_{031}\frac{1}{2}\widetilde{M}_{031} \\
&\quad + g^{12}_{031}Q_{031} \\
X^{\alpha}_{1r2} &= g^{20}_{1r2}\widetilde{N}_{1r2} + g^{30}_{1r2}\frac{3}{2}\widetilde{M}_{1r2} + g^{11}_{1r2}\frac{1}{2}N_2 + g^{21}_{1r2}Q_{1r2} \\
&\quad + g^{12}_{1r2}\frac{1}{2}M_2 \\
X^{\gamma}_{1r2} &= g^{02}_{1r2}N_2 + g^{03}_{1r2}\frac{3}{2}M_2 + g^{11}_{1r2}\frac{1}{2}\widetilde{N}_{1r2} + g^{21}_{1r2}\frac{1}{2}\widetilde{M}_{1r2} \\
&\quad + g^{12}_{1r2}Q_{1r2} \\
X^{\alpha}_{233} &= g^{20}_{233}\widetilde{N}_{233} + g^{30}_{233}\frac{3}{2}\widetilde{M}_{233} + g^{11}_{233}\frac{1}{2}N_3 + g^{21}_{233}Q_{233} \\
&\quad + g^{12}_{233}\frac{1}{2}M_3 \\
X^{\beta}_{233} &= -X^{\alpha}_{233} \\
X^{\gamma}_{233} &= g^{02}_{233}N_3 + g^{03}_{233}\frac{3}{2}M_3 + g^{11}_{233}\frac{1}{2}\widetilde{N}_{233} + g^{21}_{233}\frac{1}{2}\widetilde{M}_{233} \\
&\quad + g^{12}_{233}Q_{233} \\
X^{\alpha}_{244} &= g^{20}_{244}\widetilde{N}_{244} + g^{30}_{244}\frac{3}{2}\widetilde{M}_{244} + g^{11}_{244}\frac{1}{2}N_4 + g^{21}_{244}Q_{244} \\
&\quad + g^{12}_{244}\frac{1}{2}M_4 \\
X^{\beta}_{244} &= -X^{\alpha}_{244} \\
X^{\gamma}_{244} &= g^{02}_{244}N_4 + g^{03}_{244}\frac{3}{2}M_4 + g^{11}_{244}\frac{1}{2}\widetilde{N}_{244} + g^{21}_{244}\frac{1}{2}\widetilde{M}_{244} \\
&\quad + g^{12}_{244}Q_{244}.
\end{aligned}$$

The vectors S^h and B^h of (57) and (59) (omitted for simplicity) are formed according to the definitions of (46)–(49), (58), and (60), the corresponding (80), (81), and (89)–(102). The harmonic tones coefficients are finally computed by (68), and thus HD_2 and HD_3.

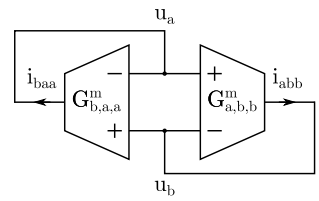

Fig. 17. Resistor as two antiparallel G_m-stages.

F. Additional Remarks

To conclude the proposed method's core section, some remarks regarding less typical circuit cases are in order.

1) Series Resistor: In a case where a resistor is in series with a capacitor (like in a Miller compensation scheme where a series resistor is included for the elimination of a possible right half-plane zero), the method's form does not feature an explicit way to account for it. However, the resistor can be replaced by the equivalent block of Fig. 17, as a G_m-stage model. If the resistor, R, placed between nodes a and b, is linear, the only nonzero coefficients of the two stages modeled by (8) are $g^{10}_{baa} = g^{10}_{abb} = 1/R$. Weak nonlinear behavior of a resistor can also be captured by including more terms of (8).

Another possible use of such a resistor formulation is to model a capacitance, C_t, at the negative input of the stage $G^m_{i,t,j}$, in the case where $k_{itj} \neq 1$. For example, if a capacitor is added at the gate of M_2 in Fig. 9, R_{L_1} can be replaced by the equivalent block of Fig. 17; then, the voltage at the gate of M_2 becomes a new variable, u_5, and stage $G^m_{0,3,1}$ changes to $G^m_{0,5,1}$, with $k_{051} = 1$.

2) Parasitic Capacitors: Parasitic capacitors can be added at any node of the G_m-stage circuit representation. Their inclusion benefits nodes where no other capacitance is present, or nodes with a very small capacitance value.

3) Process, Supply Voltage, and Temperature Variations: The method can be performed for process, supply voltage, and temperature variations (PVT), by simply repeating the derivation of the $g^{k\ell}_{itj}$-coefficients of all G_m-stages and then solving (43) and (68). The variations will have an impact on the resulting output currents of the stages, that will be captured by the newly derived $g^{k\ell}_{itj}$-coefficients. The repetition of the method is much faster than the required repetition of simulation, boosting even further the speed-up gain of the distortion estimation.

V. Simulation Results

The proposed harmonic distortion estimation method is verified by Cadence Spectre simulation in TSMC 0.18 μm technology. Supply rails are set to ± 2.5 V for all cases presented, while distortion results are obtained from parametric PSS-analysis. Each amplifier load has a reference voltage equal to the dc-operating point of its output node.

The method is implemented in MATLAB, and no parasitic capacitors are taken into account; their inclusion would result in better accuracy at high frequencies. As a rough estimate, the time of distortion estimation drops from minutes (parametric PSS-analysis) to seconds (proposed method).

A. One-Stage Cascode Amplifier

The first simulation case is that of the one-stage cascode amplifier of Fig. 15. The implemented stage has 21.56 dB dc-gain and a unity-gain frequency of 17.86 MHz, while driving a load of 10 k$\Omega \| 10$ pF. Under an input signal of 12.5 mV peak,

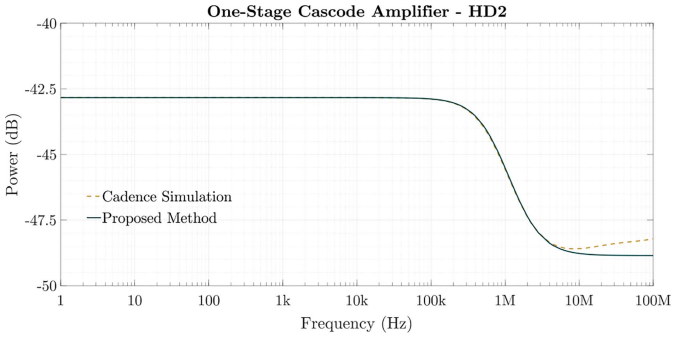

Fig. 18. HD_2 of the one-stage cascode amplifier.

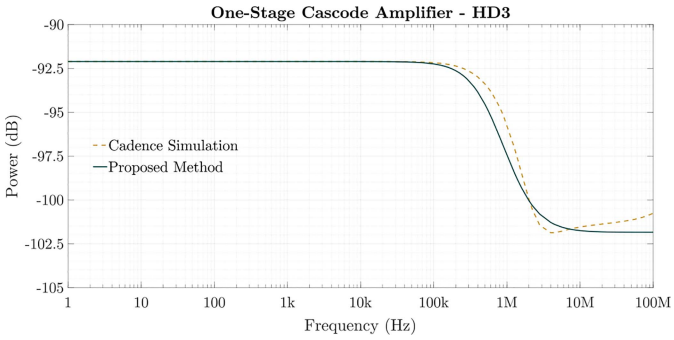

Fig. 19. HD_3 of the one-stage cascode amplifier.

the method's resulting HD_2 and HD_3 factors are presented in Figs. 18 and 19, respectively, against the results obtained by Cadence Spectre.

The results of the proposed method are in fine agreement with the simulation ones; the error between the simulation and the method is less than 0.64 dB for HD_2, and 1.75 dB for HD_3, for up to 100 MHz. For frequencies up to the unity-gain frequency of the amplifier, the HD_2 error is found to be less than 0.33 dB.

B. Three-Stage Feedback Amplifier

Next, the method is applied to the three-stage feedback amplifier of Fig. 9, that has a feedback factor of $\beta = 0.05$. The amplifier drives a load of 10 k$\Omega\|$10 pF, has a dc-gain of 26.01 dB and a unity-gain frequency of 16.80 MHz. Fig. 20 shows HD_2, with HD_3 being depicted in Fig. 21, for an input signal of 25 mV peak.

Both distortion factors predicted by the method are in excellent agreement with the ones from the simulation. Up to 100 MHz, the error is less than 1.79 dB for HD_2, and less than 1.58 dB for HD_3. Within the amplifier's unity-gain bandwidth, the maximum errors fall to 0.49 dB and 0.93 dB, respectively.

C. One-Stage Fully-Differential Amplifier

Finally, the one-stage fully-differential amplifier of Fig. 22 is simulated. The structure has 25.52 dB dc-gain and 23.79 MHz unity-gain frequency, under a load of 25 k$\Omega\|$5 pF per output. With a 25 mV peak input signal, Figs. 23 and 24 present HD_2 and HD_3, respectively.

The HD_3 factor is again in fine agreement with the corresponding simulation result; the error is found to be less than 2.36 dB for the bandwidth of 100 MHz, while within the amplifier's unity-gain frequency is less than 0.41 dB. Both

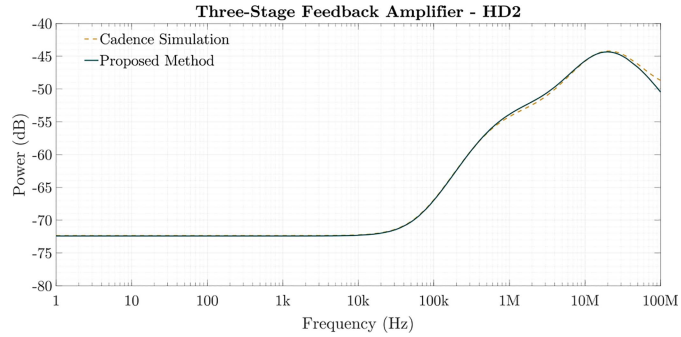

Fig. 20. HD_2 of the three-stage feedback amplifier.

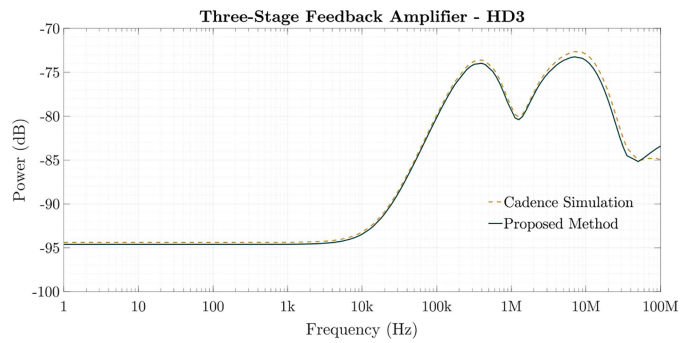

Fig. 21. HD_3 of the three-stage feedback amplifier.

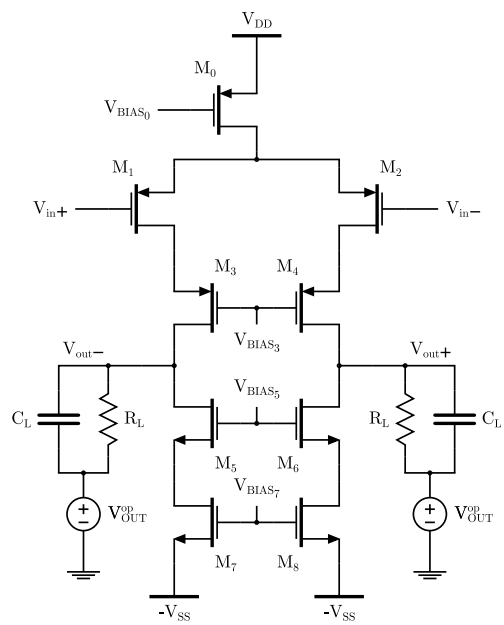

Fig. 22. One-stage fully-differential amplifier.

HD_2 estimation results indicate practically a negligible second harmonic, as is expected by the fully-differential nature of the structure.

VI. Conclusion

In this article, a time-domain harmonic distortion estimation method is presented, that can be applied systematically to CMOS circuits with any number of stages. It can be implemented in MATLAB and yields accurate distortion estimation

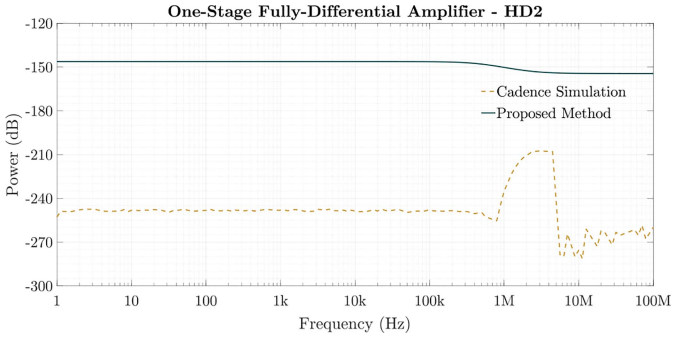

Fig. 23. HD_2 of the one-stage fully-differential amplifier.

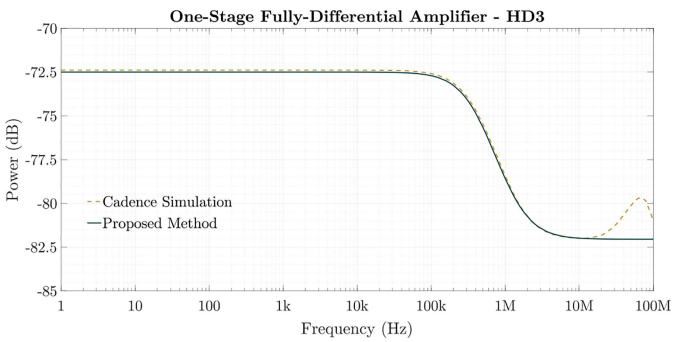

Fig. 24. HD_3 of the one-stage fully-differential amplifier.

results, verified by comparison with Cadence Spectre simulation. The method holds a fast computational profile that intends to be exploited by integration in EDA suites.

Appendix

With coefficients $\widetilde{a}_{itj,1}$, $\widetilde{b}_{itj,1}$, $a_{j,1}$, and $b_{j,1}$ known from the solution of S^f by (43), the coefficients of (46)–(49) and the matrices (103)–(107) of (50)–(52) are given by

$$\widetilde{f}^{s2}_{itj} = \widetilde{a}_{itj,1}\widetilde{b}_{itj,1} \tag{89}$$

$$\widetilde{f}^{c2}_{itj} = \frac{-\widetilde{a}^2_{itj,1} + \widetilde{b}^2_{itj,1}}{2} \tag{90}$$

$$\widetilde{f}^{s3}_{itj} = \frac{\widetilde{a}_{itj,1}}{4}\left(-\widetilde{a}^2_{itj,1} + 3\widetilde{b}^2_{itj,1}\right) \tag{91}$$

$$\widetilde{f}^{c3}_{itj} = \frac{\widetilde{b}_{itj,1}}{4}\left(-3\widetilde{a}^2_{itj,1} + \widetilde{b}^2_{itj,1}\right) \tag{92}$$

$$f^{s2}_{j} = a_{j,1}b_{j,1} \tag{93}$$

$$f^{c2}_{j} = \frac{-a^2_{j,1} + b^2_{j,1}}{2} \tag{94}$$

$$f^{s3}_{j} = \frac{a_{j,1}}{4}\left(-a^2_{j,1} + 3b^2_{j,1}\right) \tag{95}$$

$$f^{c3}_{j} = \frac{b_{j,1}}{4}\left(-3a^2_{j,1} + b^2_{j,1}\right) \tag{96}$$

$$h^{s2}_{itj} = \frac{\widetilde{a}_{itj,1}b_{j,1} + \widetilde{b}_{itj,1}a_{j,1}}{2} \tag{97}$$

$$h^{c2}_{itj} = \frac{-\widetilde{a}_{itj,1}a_{j,1} + \widetilde{b}_{itj,1}b_{j,1}}{2} \tag{98}$$

$$r^{s3}_{itj} = \left(-\widetilde{a}^2_{itj,1} + \widetilde{b}^2_{itj,1}\right)\frac{a_{j,1}}{4} + \left(\widetilde{a}_{itj,1}\widetilde{b}_{itj,1}\right)\frac{b_{j,1}}{2} \tag{99}$$

$$r^{c3}_{itj} = \left(-\widetilde{a}^2_{itj,1} + \widetilde{b}^2_{ijt,1}\right)\frac{b_{j,1}}{4} - \left(\widetilde{a}_{itj,1}\widetilde{b}_{itj,1}\right)\frac{a_{j,1}}{2} \tag{100}$$

$$o^{s3}_{itj} = \left(-a^2_{j,1} + b^2_{j,1}\right)\frac{\widetilde{a}_{itj,1}}{4} + \left(a_{j,1}b_{j,1}\right)\frac{\widetilde{b}_{itj,1}}{2} \tag{101}$$

$$o^{c3}_{itj} = \left(-a^2_{j,1} + b^2_{j,1}\right)\frac{\widetilde{b}_{itj,1}}{4} - \left(a_{j,1}b_{j,1}\right)\frac{\widetilde{a}_{itj,1}}{2} \tag{102}$$

$$\widetilde{N}_{itj} = \begin{bmatrix} 0 & 0 & \widetilde{b}_{itj,1} & -\widetilde{a}_{itj,1} \\ 0 & 0 & \widetilde{a}_{itj,1} & \widetilde{b}_{itj,1} \\ \widetilde{b}_{itj,1} & \widetilde{a}_{itj,1} & 0 & 0 \\ -\widetilde{a}_{itj,1} & \widetilde{b}_{itj,1} & 0 & 0 \end{bmatrix} \in \mathbb{R}^{4\times 4} \tag{103}$$

$$N_j = \begin{bmatrix} 0 & 0 & b_{j,1} & -a_{j,1} \\ 0 & 0 & a_{j,1} & b_{j,1} \\ b_{j,1} & a_{j,1} & 0 & 0 \\ -a_{j,1} & b_{j,1} & 0 & 0 \end{bmatrix} \in \mathbb{R}^{4\times 4} \tag{104}$$

$$\widetilde{M}_{itj} = \left(\widetilde{a}^2_{itj,1} + \widetilde{b}^2_{itj,1}\right)I_4 \in \mathbb{R}^{4\times 4} \tag{105}$$

$$M_j = \left(a^2_{j,1} + b^2_{j,1}\right)I_4 \in \mathbb{R}^{4\times 4} \tag{106}$$

$$Q_{itj} = \left(\widetilde{a}_{itj,1}a_{j,1} + \widetilde{b}_{itj,1}b_{j,1}\right)I_4 \in \mathbb{R}^{4\times 4}. \tag{107}$$

References

[1] T. C. Carusone, D. Johns, and K. Martin, *Analog Integrated Circuit Design*, 2nd ed. Hoboken, NJ, USA: Wiley, 2011.

[2] D. Self, *Audio Power Amplifier Design*, 6th ed. New York, NY, USA: Focal Press, 2013.

[3] P. Dobrovolny, G. Vandersteen, P. Wambacq, and S. Donnay, "Analysis and compact behavioral modeling of nonlinear distortion in analog communication circuits," *IEEE Trans. Comput.-Aided Design Integr. Circuits Syst.*, vol. 22, no. 9, pp. 1215–1227, Sep. 2003.

[4] R. J. Gilmore and M. B. Steer, "Nonlinear circuit analysis using the method of harmonic balance—A review of the art. Part I. Introductory concepts," *Int. J. Microw. Millimeter Wave Comput.-Aided Eng.*, vol. 1, no. 1, pp. 22–37, 1991.

[5] S. A. Maas, *Nonlinear Microwave and RF Circuits*, 2nd ed. Boston, MA, USA: Artech House, 2003.

[6] D. Tannir and R. Khazaka, "Adjoint sensitivity analysis of nonlinear distortion in radio frequency circuits," *IEEE Trans. Comput.-Aided Design Integr. Circuits Syst.*, vol. 30, no. 6, pp. 934–939, Jun. 2011.

[7] D. Tannir, "Direct sensitivity analysis of nonlinear distortion in RF circuits using multidimensional moments," *IEEE Trans. Comput.-Aided Design Integr. Circuits Syst.*, vol. 34, no. 3, pp. 321–331, Mar. 2015.

[8] P. Wambacq and W. Sansen, *Distortion Analysis of Analog Integrated Circuits* (The Springer International Series in Engineering and Computer Science), 1st ed. Boston, MA, USA: Springer, 1998, vol. 451.

[9] P. Li and L. T. Pileggi, "Efficient per-nonlinearity distortion analysis for analog and RF circuits," *IEEE Trans. Comput.-Aided Design Integr. Circuits Syst.*, vol. 22, no. 10, pp. 1297–1309, Oct. 2003.

[10] Z. Zhang, A. Celik, and P. Sotiriadis, "A fast state-space algorithm to estimate harmonic distortion in fully differential weakly nonlinear g_m-c filters," in *Proc. IEEE Int. Symp. Circuits Syst. (ISCAS)*, Kos, Greece, May 2006, pp. 2954–2956.

[11] Z. Zhang, A. Celik, and P. P. Sotiriadis, "State-space harmonic distortion modeling in weakly nonlinear, fully balanced g_m-c filters-a modular approach resulting in closed-form solutions," *IEEE Trans. Circuits Syst. I. Reg. Papers*, vol. 53, no. 1, pp. 48–59, Jan. 2006.

[12] P. P. Sotiriadis, A. Celik, D. Loizos, and Z. Zhang, "Fast state-space harmonic-distortion estimation in weakly nonlinear g_m-c filters," *IEEE Trans. Circuits Syst. I, Reg. Papers*, vol. 54, no. 1, pp. 218–228, Jan. 2007.

[13] A. Cooman, P. Bronders, D. Peumans, G. Vandersteen, and Y. Rolain, "Distortion contribution analysis with the best linear approximation," *IEEE Trans. Circuits. Syst. I, Reg. Papers*, vol. 65, no. 12, pp. 4133–4146, Dec. 2018.

[14] Y. Miao and Y. Zhang, "Distortion modeling of feedback two-stage amplifier compensated with miller capacitor and nulling resistor," *IEEE Trans. Circuits Syst. I, Reg. Papers*, vol. 59, no. 1, pp. 93–105, Jan. 2012.

[15] G. Shi, "Symbolic distortion analysis of multistage amplifiers," *IEEE Trans. Circuits Syst. I, Reg. Papers*, vol. 66, no. 1, pp. 369–382, Jan. 2019.

[16] G. Palumbo and S. Pennisi, "Feedback amplifiers: A simplified analysis of harmonic distortion in the frequency domain," in *Proc. 8th IEEE Int. Conf. Electron. Circuits Syst. (Cat.No.01EX483)*, vol. 1. Valletta, Malta, Sep. 2001, pp. 209–212.

[17] G. Giustolisi, G. Palumbo, and S. Pennisi, "Harmonic distortion in single-stage amplifiers," in *Proc. IEEE Int. Symp. Circuits Syst. (Cat. No.02CH37353)*, vol. 2. Scottsdale, AZ, USA, May 2002, pp. 33–36.

[18] G. Palumbo and S. Pennisi, "High-frequency harmonic distortion in feedback amplifiers: Analysis and applications," *IEEE Trans. Circuits Syst. I, Fundam. Theory Appl.*, vol. 50, no. 3, pp. 328–340, Mar. 2003.

[19] G. Palumbo and S. Pennisi, "Harmonic distortion in three-stage nested-miller-compensated amplifiers," in *Proc. IEEE Int. Symp. Circuits Syst. (IEEE Cat. No.04CH37512)*, vol. 1. Vancouver, BC, Canada, May 2004, pp. 485–488.

[20] S. O. Cannizzaro, G. Palumbo, and S. Pennisi, "Accurate estimation of high-frequency harmonic distortion in two-stage miller OTAs," *IEE Proc. Circuits Devices Syst.*, vol. 152, no. 5, pp. 417–424, Oct. 2005.

[21] S. O. Cannizzaro, G. Palumbo, and S. Pennisi, "Distortion analysis of three-stage amplifiers with reversed nested-miller compensation," in *Proc. Eur. Conf. Circuit Theory Design*, vol. 3. Cork, Ireland, Sep. 2005, pp. III/93–III/96.

[22] S. O. Cannizzaro, G. Palumbo, and S. Pennisi, "New analytical approach to evaluate harmonic distortion in nonlinear feedback amplifiers," in *Proc. Eur. Conf. Circuit Theory Design*, vol. 3. Cork, Ireland, Sep. 2005, pp. III/97–III/100.

[23] S. O. Cannizzaro, G. Palumbo, and S. Pennisi, "Distortion analysis of miller-compensated three-stage amplifiers," *IEEE Trans. Circuits Syst. I, Reg. Papers*, vol. 53, no. 5, pp. 961–976, May 2006.

[24] S. O. Cannizzaro, G. Palumbo, and S. Pennisi, "An approach to model high-frequency distortion in negative-feedback amplifiers," *Int. J. Circuit Theory Appl.*, vol. 36, no. 1, pp. 3–18, 2008.

[25] A. Borys, "On analysis of harmonic distortion in op amps based circuits via volterra series," in *Proc. 23rd Int. Conf. Mixed Design Integr. Circuits Syst. (MIXDES)*, Lodz, Poland, Jun. 2016, pp. 330–335.

[26] D. Baxevanakis and P. P. Sotiriadis, "Accurate harmonic distortion estimation in CMOS circuits using a cross-product g_m-stage modeling," in *Proc. IEEE Int. Symp. Circuits Syst. (ISCAS)*, 2020, pp. 1–5.

[27] S. Kang, B. Choi, and B. Kim, "Linearity analysis of CMOS for RF application," *IEEE Trans. Microw. Theory Techn.*, vol. 51, no. 3, pp. 972–977, Mar. 2003.

[28] B. Toole, C. Plett, and M. Cloutier, "RF circuit implications of moderate inversion enhanced linear region in mosfets," *IEEE Trans. Circuits Syst. I, Reg. Papers*, vol. 51, no. 2, pp. 319–328, Feb. 2004.

[29] B. Hernes and W. Sansen, "Distortion in single-, two- and three-stage amplifiers," *IEEE Trans. Circuits Syst. I, Reg. Papers*, vol. 52, no. 5, pp. 846–856, May 2005.

[30] S. C. Blaakmeer, E. A. M. Klumperink, D. M. W. Leenaerts, and B. Nauta, "Wideband Balun-LNA with simultaneous output balancing, noise-canceling and distortion-canceling," *IEEE J. Solid-State Circuits*, vol. 43, no. 6, pp. 1341–1350, Jun. 2008.

[31] P. S. Crovetti, "Finite common-mode rejection in fully differential nonlinear circuits," *IEEE Trans. Circuits Syst. II, Exp. Briefs*, vol. 58, no. 8, pp. 507–511, Aug. 2011.

[32] P. S. Crovetti and F. Fiori, "Finite common-mode rejection in fully differential operational amplifiers," *Electron. Lett.*, vol. 42, no. 11, pp. 615–617, May 2006.

[33] F. Fiori and P. S. Crovetti, "Nonlinear effects of radio-frequency interference in operational amplifiers," *IEEE Trans. Circuits Syst. I, Fundam. Theory Appl.*, vol. 49, no. 3, pp. 367–372, Mar. 2002.

[34] B. Perez-Verdu, J. Cruz, B. Linares-Barranco, A. Rodriguez-Vazquez, J. L. Huertas, and E. Sanchez-Sinencio, "Nonlinear time-domain macromodeling of OTA circuits," in *Proc. IEEE Int. Symp. Circuits Syst.*, vol. 2. Portland, OR, USA, May 1989, pp. 1441–1444.

[35] N. Scheinberg and A. Pinkhasov, "A computer simulation model for simulating distortion in FET resistors," *IEEE Trans. Comput.-Aided Design Integr. Circuits Syst.*, vol. 19, no. 9, pp. 981–989, Sep. 2000.

[36] H. W. Sorenson, *Parameter Estimation: Principles and Problems* (Control and Systems Theory), vol. 9. New York, NY, USA: M. Dekker, 1980.

[37] P. Lancaster and M. Tismenetsky, *The Theory of Matrices With Applications* (Computer Science and Scientific Computing), 2nd ed. New York, NY, USA: Academic, 1985.

[38] R. A. Horn and C. R. Johnson, *Matrix Analysis*, 2nd ed. New York, NY, USA: Cambridge Univ. Press, 2013.

Dimitrios Baxevanakis (Graduate Student Member, IEEE) received the Diploma degree in electrical and computer engineering from the National Technical University of Athens, Greece, in 2016, where he is currently pursuing the Ph.D. degree under the supervision of Prof. P. P. Sotiriadis.

He is a Teaching Assistant in undergraduate and graduate courses and acts as an Advisor in diploma theses. He has authored and coauthored several conference papers and journal articles. His main research interests include analog microelectronic circuits, high-linearity and high-efficiency output stages, power converters, distortion analysis, and systems and control.

Mr. Baxevanakis is a member of the Technical Chamber of Greece, and a regular reviewer for many IEEE conference and journal publications.

Paul P. Sotiriadis (Senior Member, IEEE) received the Diploma degree from the Electrical and Computer Engineering Department, Stanford University, Stanford, CA, USA, the M.S. degree in electrical engineering from Stanford University, and the Ph.D. degree in electrical engineering and computer science from the Massachusetts Institute of Technology, Cambridge, MA, USA, in 2002.

He is a Faculty Member of the Electrical and Computer Engineering Department, National Technical University of Athens, Greece, where he is the Director of the Electronics Laboratory, and a Member of the Governing Board of the Hellenic Space Center, National Space Center of Greece. In 2002, he joined the Johns Hopkins University, Baltimore, MD, USA, as an Assistant Professor of electrical and computer engineering. In 2012, he joined the faculty of the Electrical and Computer Engineering Department, National Technical University of Athens. He has authored and coauthored more than 150 research publications, most of them in IEEE journals and conferences, holds one patent, and has contributed chapters to technical books. He has led several projects in these fields funded by U.S. organizations and has collaborations with industry and national labs. His research interests include design, optimization, and mathematical modeling of analog and mixed-signal circuits, RF and microwave circuits, advanced frequency synthesis, biomedical instrumentation, and interconnect networks in deep-submicrometer technologies.

Dr. Sotiriadis has received several awards, including the 2012 Guillemin-Cauer Award from the IEEE Circuits and Systems Society, the Best Paper Award in the IEEE International Symposium on Circuits and Systems 2007, the Best Paper Award in the IEEE International Frequency Control Symposium 2012, and the Best Paper Award in the IEEE International Conference on Modern Circuits and Systems Technologies 2019. He is an Associate Editor of the IEEE SENSORS JOURNAL, has served as an Associate Editor of the IEEE TRANSACTIONS ON CIRCUITS AND SYSTEMS I: REGULAR PAPERS from 2016 to 2020, and the IEEE TRANSACTIONS ON CIRCUITS AND SYSTEMS II: EXPRESS BRIEFS from 2005 to 2010, and has been a member of technical committees of many conferences. He regularly reviews for many IEEE transactions and conferences and serves on proposal review panels.